Chapter 2
Forced Vibrations of Damped Non-homogeneous Timoshenko Beams

Arnaldo J. Mazzei

Abstract This work is the next of a series on vibrations of non-homogeneous structures. It addresses the lateral harmonic forcing, with spatial dependencies, of a two-segment damped Timoshenko beam. In the series, frequency response functions (FRFs) were determined for segmented structures, such as rods and beams, using analytic and numerical approaches. These structures are composed of stacked cells, which are made of different materials and may have different geometric properties. The goal is the determination of frequency response functions (FRFs). Two approaches are employed. The first approach uses displacement differential equations for each segment, where boundary and interface continuity conditions are used to determine the constants involved in the solutions. Then the response, as a function of forcing frequency, can be obtained. This procedure is unwieldy, and determining particular integrals can become difficult for arbitrary spatial variations. The second approach uses logistic functions to model segment discontinuities. The result is a system of partial differential equations with variable coefficients. Numerical solutions are developed with the aid of MAPLE® software. For free/fixed boundary conditions, spatially constant force, and viscous damping, excellent agreement is found between the methods. The numerical approach is then used to obtain FRFs for cases including spatially varying load.

Keywords Layered structures · Logistic functions · Non-homogenous structures FRFs · Timoshenko damped beam

Nomenclature

A	Cross-section area (A_i, cross-section area for i-th material)
C_{Ti}, C_{Ri}	Viscous damping coefficients per unit length
C_i	Non-dimensional damping coefficients
D_{ij}	Proportional damping matrix coefficients
E	Young's modulus (E_i, Young's modulus for i-th material)
f_i	Non-dimensional logistic functions
G_i	Beam segment material shear modulus
I	Area moment of inertia of the beam cross-section (I_i, moment of inertia of i-cell)
k	Shear coefficient (k_i, shear coefficient of i-cell)
K	Non-dimensional logistic function parameter
K_{ij}	Stiffness matrix coefficients
L	Length of beam (L_i, length of i-th cell)
M	Bending moment
M_{ij}	Mass matrix coefficients
P_i	Generalized external forces
p_i	Force acting on the i-segment
Q	Non-dimensional forcing function
q	External force per unit length acting on the beam
q_1	Spatial forcing function for harmonic solution
r_1, s_1	Shape function constants
t	Time
$\hat{U}_i$, $\hat{V}_i$	Generalized coordinates
V	Shear force
x	Longitudinal coordinate

A. J. Mazzei (✉)
Department of Mechanical Engineering, C. S. Mott Engineering and Science Center, Kettering University, Flint, MI, USA
e-mail: amazzei@kettering.edu

C. Walber et al. (eds.), *Sensors and Instrumentation, Aircraft/Aerospace and Dynamic Environments Testing, Volume 7*,
Conference Proceedings of the Society for Experimental Mechanics Series, https://doi.org/10.1007/978-3-031-05415-0_2

w	Transverse displacement of the beam
Y	Non-dimensional transverse displacement of the beam, $Y = w/L$
Z, ϕ	Spatial functions for harmonic solution
α, β	Constants of mass and stiffness proportionality
α_1, γ_1	Non-dimensional parameters
γ	Shear strain
δ_j	Cell properties
ζ_i	Modal damping ratio
θ	Rotational angle of the beam cross-section
$\hat{\lambda}$	Complex frequency, $\hat{\lambda} = (a + bI)$
λ_i, η_i	Shape functions
ν	Non-dimensional frequency, $\nu = \Omega/\Omega_0$
ξ	Non-dimensional spatial coordinate, $\xi = x/L$
ρ	Mass density (ρ_i, density value for i-th material)
τ	Non-dimensional time, $\tau = \Omega_0 t$
υ_i	Beam segment material Poisson's ratio
Ω_0	Reference frequency

2.1 Introduction

This work adds to a series (see Refs. [1–3]) on transverse vibrations of layered beams. The main interest is the vibration analysis, both theoretical and numerical, of segmented damped beams. The media are structures with different materials and varying cross-sections, which are layered in cells and may be uniform or not.

The objective is the determination of frequency response functions (FRFs). Timoshenko beam theory is used for a two-segment configuration under harmonic forcing.

Two approaches are used to address the problem. In the first, analytic solutions are derived for the differential equations for each segment. The constants involved are determined using boundary and interface continuity conditions. The response, at a given location, can then be obtained as a function of forcing frequency (FRF). Note that the procedure can become unwieldy for arbitrary spatial variations. In the second, the discrete cell properties are modeled by continuously varying functions, specifically logistic functions. This provides for a system of differential equations with variable coefficients. The system is then solved numerically utilizing MAPLE®[1] software.

Similar analytical and numerical approaches were applied in Refs. [1–3] (Euler-Bernoulli and Timoshenko models). Overall results showed that the numerical method worked very well when compared to the analytical solutions.

A brief literature review is given next.

For vibrations of layered beams, one may refer to the list given in Refs. [1–3]. Solids composed by discrete layers are studied in Refs. [4–7]. Reference [8] provides a review of articles on this subject.

Reference [9] treats damping effects on Timoshenko beams. The numerical analyses allowed for outlining the relevant influences on the dynamic response associated with any singular damping mechanism and the evaluation of the modal critical damping values. In Ref. [10] a generalized Fourier analysis is applied to damped Timoshenko beam equation to evaluate displacements and bending stresses from random loading. Some of the models were found to be adequate for that purpose. In Ref. [11] the equations of motion for a non-uniform damped Timoshenko beam with distributed axial force are used to extract principal modes of vibration, by numerical means and for specific boundary and orthogonality conditions. Reference [12] deals with Timoshenko beam equations with external damping and internal damping terms plus forcing terms. Different boundary conditions such as pinned ends, hinged-sliding ends, and sliding ends are considered. Unboundedness of solutions of boundary value problems is studied, and it is shown that the magnitude of the displacement of the beam grows up to ∞ as $t \to \infty$ under some assumptions on the forcing term. In Ref. [13], the dynamic behavior of nonlocal viscoelastic damped nanobeams is studied. A Kelvin–Voigt viscoelastic model, velocity-dependent external damping, and Timoshenko beam theory are employed to establish the governing equations and boundary conditions for the vibration of nanotubes. Using transfer function methods (TFMs), the natural frequencies and frequency response functions (FRF) are calculated for different boundary conditions. Reference [14] investigates the effects of axial compressive load and internal viscous damping on the free vibration characteristics of Timoshenko beams using the dynamic stiffness formulation and the differential transformation method. A dynamic stiffness method (DSM) is used where the dynamic stiffness matrix of an axially loaded Timoshenko beam with internal viscous damping is constructed to calculate natural frequencies. The numerical

[1] www.maplesoft.com

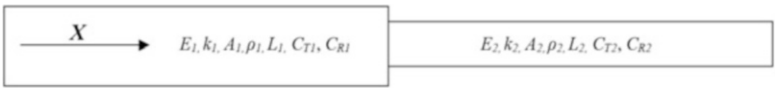

Fig. 2.1 Layered beam

approach compares well to the analytical solutions. Parametric studies on vibrations of twisted Timoshenko damped beams are given in Ref. [15]. Using Timoshenko beam theory and Hamilton's principle, bending–bending vibrations of axially loaded twisted beams with locally distributed Kelvin–Voigt damping are analyzed. A finite element method is used to reduce the equations of motion into linear second-order ordinary differential equations with constant coefficients. It was asserted that the approach led to a better understanding of the variables affecting the beam vibration characteristics.

2.2 Basic Structure

The segmented beam is shown in Fig. 2.1. It is composed of two cells of different materials. E, ρ, and A may vary in a discontinuous manner. The segments are under transverse loads q_1 and q_2 (force per unit length) and viscous damping forces due to translation and rotation of the cross-section during deflection (per unit length, damping coefficients C_{T1}, C_{R1}, and C_{T2}, C_{R2}).

The equations of motion for a transversely loaded, viscously damped Timoshenko beam are given below. (Details for deriving the equations are discussed in Ref. [2]; see also Refs. [11, 16]). A displacement-velocity and rotation-velocity–dependent viscous damping model is used [13]:

$$\begin{aligned}
&\rho(x)\ A(x)\ \frac{\partial^2 w(x,t)}{\partial t^2} + C_{\mathrm{T}}(x)\frac{\partial w(x,t)}{\partial t} - \frac{\partial V}{\partial x} = q\ (x,t)\\
&\rho(x)\ I(x)\frac{\partial^2 \theta(x,t)}{\partial t^2} + C_{\mathrm{R}}(x)\frac{\partial \theta(x,t)}{\partial t} + \frac{\partial M}{\partial x} - V = 0
\end{aligned} \tag{2.1}$$

Using a linearized curvature model, Eq. (2.1) can be re-written as:

$$\begin{aligned}
&\rho(x)A(x)\ \frac{\partial^2 w(x,t)}{\partial t^2} + C_{\mathrm{T}}(x)\frac{\partial w(x,t)}{\partial t} = q\ (x,t) + \frac{\partial}{\partial x}\left[kA(x)G(x)\left(\frac{\partial w(x,t)}{\partial t} - \theta\ (x,t)\right)\right]\\
&\rho(x)I(x)\frac{\partial^2 \theta(x,t)}{\partial t^2} + C_{\mathrm{R}}(x)\frac{\partial \theta(x,t)}{\partial t} = \frac{\partial}{\partial x}\left[E(x)I(x)\frac{\partial \theta(x,t)}{\partial x}\right] + kA(x)G(x)\left(\frac{\partial w(x,t)}{\partial t} - \theta\ (x,t)\right)
\end{aligned} \tag{2.2}$$

In Eq. (2.2) the shear force is given by $V = kA(x)G(x)\gamma$, where k is the "shear coefficient" (see Ref. [17]), which relates the maximum shear stress to the average value in the cross-section of the beam. Also, $\frac{\partial w}{\partial x} = \theta + \gamma$ and $M = -\mathrm{EI}\frac{\partial \theta}{\partial x}$.

Approaches for obtaining the steady-state response, due to harmonic forcing, are sought next.

2.3 Solution Approaches

Non-dimensional versions of Eq. (2.2) can be obtained by taking $\tau = \Omega_0 t$, $\nu = \frac{\Omega}{\Omega_0}$, $\xi = \frac{x}{L}$, $Y = \frac{w}{L}$, $E(x) = E_1 f_1(\xi)$, $I(x) = I_1 f_2(\xi)$, $\rho(x) = \rho_1 f_3(\xi)$, $A(x) = A_1 f_4(\xi)$, and $kG(x) = k_1 G_1 f_5(\xi)$. This leads to:

$$\begin{aligned}
&f_3\ (\xi)\, f_4\ (\xi)\ \frac{\partial^2 Y(\xi,\tau)}{\partial \tau^2} + C_1(x)\frac{\partial Y(\xi,\tau)}{\partial \tau} = Q\ (\xi,\tau) + \alpha_1 \frac{\partial}{\partial \xi}\left(f_4\ (\xi) f_5\ (\xi)\left(\frac{\partial Y(\xi,\tau)}{\partial \xi} - \theta\ (\xi,\tau)\right)\right)\\
&f_3\ (\xi)\, f_2\ (\xi)\ \frac{\partial^2 \theta(\xi,\tau)}{\partial \tau^2} + C_2(x)\frac{\partial \theta(\xi,\tau)}{\partial \tau} = \gamma_1 \frac{\partial}{\partial \xi}\left(f_1\ (\xi)\ f_2\ (\xi)\ \frac{\partial \theta(\xi,\tau)}{\partial \xi}\right) + (\alpha_1\gamma_1 f_4\ (\xi) f_5\ (\xi))\left(\frac{\partial Y(\xi,\tau)}{\partial \xi} - \theta\ (\xi,\tau)\right)
\end{aligned} \tag{2.3}$$

where $\Omega_0 = \sqrt{\frac{E_1 I_1}{\rho_1 A_1 L^4}}$ (reference frequency), $C_1 = C_T\sqrt{\frac{L^4}{\rho_1 A_1 E_1 I_1}}$, $C_2 = C_R\sqrt{\frac{A_1 L^4}{\rho_1 E_1 {I_1}^3}}$, $Q\ (\xi,\tau) = q\ (x,t)\ \frac{L^3}{E_1 I_1}$, $\alpha_1 = \frac{k_1 G_1 A_1 L^2}{E_1 I_1}$, and $\gamma_1 = \frac{A_1 L^2}{I_1}$. f_i are functions representing the transitions from one cell to another. (For the continuous variation approach, logistic functions will be utilized; details are given below.)

Assuming harmonic forcing with frequency $\hat{\lambda}$, $Q(\xi,\tau) = q_1(\xi)\exp\left(\hat{\lambda}\tau\right)$, one can take $Y(\xi,\tau) = Z(\xi)\exp\left(\hat{\lambda}\tau\right)$ and $\theta(\xi,\tau) = \phi(\xi)\exp\left(\hat{\lambda}\tau\right)$. This leads to:

$$\begin{array}{l} f_3(\xi) f_4(\xi)\ \hat{\lambda}^2 Z(\xi) + C_1\hat{\lambda} Z(\xi) - \alpha_1 \frac{d}{d\xi}\left(f_4(\xi) f_5(\xi)\left(\frac{dZ(\xi)}{d\xi} - \phi(\xi)\right)\right) - q_1(\xi) = 0 \\ f_3(\xi) f_2(\xi)\ \hat{\lambda}^2\phi(\xi) + C_2\hat{\lambda}\phi(\xi) - \gamma_1 \frac{d}{d\xi}\left(f_1(\xi) f_2(\xi)\frac{d\phi(\xi)}{d\xi}\right) - (\alpha_1\gamma_1 f_4(\xi) f_5(\xi))\left(\frac{dZ(\xi)}{d\xi} - \phi(\xi)\right) = 0 \end{array} \tag{2.4}$$

Taking $\hat{\lambda} = (a + bI)$ and separating real and imaginary parts, after some manipulation, gives:

$$\begin{array}{l} \left(f_3(\xi) f_4(\xi) b^2 + \frac{{C_1}^2}{4 f_3(\xi) f_4(\xi)}\right) Z(\xi) + \alpha_1 \frac{d}{d\xi}\left(f_4(\xi) f_5(\xi)\left(\frac{dZ(\xi)}{d\xi} - \phi(\xi)\right)\right) + q_1(\xi) = 0 \\ \left(f_3(\xi) f_2(\xi) b^2 + \frac{{C_2}^2}{4 f_3(\xi) f_2(\xi)}\right)\phi(\xi) + \gamma_1 \frac{d}{d\xi}\left(f_1(\xi) f_2(\xi)\frac{d\phi(\xi)}{d\xi}\right) + (\alpha_1\gamma_1 f_4(\xi) f_5(\xi))\left(\frac{dZ(\xi)}{d\xi} - \phi(\xi)\right) = 0 \end{array} \tag{2.5}$$

The result, Eq. (2.5), is a set of non-homogeneous ordinary differential equations with variable coefficients. Analytic and numerical solutions are discussed next.

2.3.1 Analytical Approach

For constant properties in each segment, Eq. (2.5) can be written as:

$$\begin{array}{l} \left(f_3 f_4 b^2 + \frac{{C_1}^2}{4 f_3 f_4}\right) Z(\xi) + \alpha_1 f_4 f_5 \frac{d}{d\xi}\left(\left(\frac{dZ(\xi)}{d\xi} - \phi(\xi)\right)\right) + q_1(\xi) = 0 \\ \left(f_3 f_2 b^2 + \frac{{C_2}^2}{4 f_3 f_2}\right)\phi(\xi) + \gamma_1 f_1 f_2 \frac{d^2\phi(\xi)}{d\xi^2} + (\alpha_1\gamma_1 f_4 f_5)\left(\frac{dZ(\xi)}{d\xi} - \phi(\xi)\right) = 0 \end{array} \tag{2.6}$$

Note that, for the beam segments, the functions f_i are constants and can be calculated from:

$$\begin{array}{l} f_{k,i} = 1,\ k = 1\cdots 5,\quad i = 1 \\ f_{1,i} = \frac{E_i}{E_{i-1}},\ f_{2,i} = \frac{I_i}{I_{i-1}},\ f_{3,i} = \frac{\rho_i}{\rho_{i-1}},\ f_{4,i} = \frac{A_i}{A_{i-1}},\ f_{5,i} = \frac{K_i G_i}{K_{i-1} G_{i-1}},\ i = 2\cdots n \end{array} \tag{2.7}$$

Equations (2.6) and (2.7) are valid for cases with multiple segments (n).

Solutions to the system of ODEs (2.6), with constant coefficients, involve solutions to the homogeneous equations and particular integrals. Depending on the forcing function $q_1(\xi)$, tracking particular solutions may pose a problem. In this section attention is directed to obtaining solutions for the case of constant spatial forcing. (Non-constant spatial forcing is treated later numerically.)

Here this is done using MAPLE®. The solutions consist of exponential functions containing unknown coefficients, which must be determined based on the set of boundary conditions for the problem. In addition, solutions must match at the interface between the elements. Interface continuity requires matching of displacement, slope, moment, and shear force.

These conditions provide a set of algebraic equations for the unknown coefficients. The FRFs can then be obtained by monitoring solutions, for different values of the forcing frequency b, at a specific point of the beam (here this is taken at the center).

Solutions require that the boundary conditions be defined. Two sets are discussed below.

2.3.2 Numerical Approach

For the numerical approach, a continuous variation model is used. With this model, transitions from one cell to another are modeled via logistic functions. Here these functions, f_i, in non-dimensional form are taken to be:

$$f_i(\xi) = 1 + \left(\frac{\delta_2 - \delta_1}{\delta_1}\right)\left(\frac{1}{2} + \frac{1}{2}\tanh\left(K\left(\xi - \frac{1}{2}\right)\right)\right), i = 1, 2, 3, 4, 5 \tag{2.8}$$

δ_j represents a material property, geometric property, or damping (E, I, ρ, kG, A, or C). K controls the sharpness of the transition from one cell to another in the function. A larger value corresponds to a sharper transition at $\xi = \frac{1}{2}$.

Substituting Eqs. (2.8) into (2.5) leads to a system of differential equations, with variable coefficients, which may not have analytic solutions. Given the material layout and cross-section variation, i.e., the corresponding logistic functions, a MAPLE® routine can be used to obtain numerical approximations to the FRF of the system. This is done by monitoring the response for different values of the frequency b. Resonances can also be obtained via a forced-motion approach (see Ref. [18]). It consists of using MAPLE®'s two-point boundary value solver to solve a forced-motion problem. A constant value for the forcing function G is assumed and the frequency b is varied. By observing the mid-span deflection of the beam, resonant frequencies can be found on noting where changes in sign occur.

The approaches are illustrated in the following numerical examples.

2.4 Numerical Examples

Consider the beam shown in Fig. 2.1. Here the segment cross-sections are assumed to have the same geometry and to be joined at the center of the beam. The cross-section is taken to be a *S 24 X 121* (ASTM A6 – American Standard Beam),[2] and the following materials are used: aluminum ($E_1 = 71$ GPa, $\rho_1 = 2710$ Kg/m^3, $\upsilon_1 = 0.33$, $G_1 = 26.69$ GPa, $k_1 = 0.89$) and silicon carbide ($E_2 = 210$ GPa, $\rho_2 = 3100$ Kg/m^3, $\upsilon_2 = 0.16$, $G_2 = 90.52$ GPa, $k_2 = 0.87$). These values are taken from Refs. [17, 19].

2.4.1 Free/Fixed Boundary Conditions

Consider a free/fixed set. The boundary conditions are as follows (i subscript refers to the segment number).

The moment and shear free end at $\xi = 0$ gives $\frac{d\phi_1(\xi)}{d\xi}\Big|_{x=0} = 0$ and $\frac{dZ_1(\xi)}{d\xi}\Big|_{\xi=0} = \phi_1(\xi)$. The conditions at the fixed end give: $Z_2(\xi) = 0$ and $\phi_2(\xi) = 0$. Interface continuity conditions are $Z_1(\xi) = Z_2(\xi)$, $\xi = 0.5$ (displacement continuity), $\phi_1(\xi) = \phi_2(\xi)$, $\xi = 0.5$ (slope continuity), $\frac{d\phi_1(\xi)}{d\xi} = f_1 f_2 \frac{d\phi_2(\xi)}{d\xi}$, $\xi = 0.5$ (moment continuity), and $\left(\frac{dZ_1(\xi)}{d\xi} - \phi_1(\xi)\right) = f_4 f_5 \left(\frac{dZ_2(\xi)}{d\xi} - \phi_2(\xi)\right)$, $\xi = 0.5$ (shear continuity). $q_1(\xi)$ is set to 1.

Utilizing the analytical approach described above allows for the calculation of the FRF for the system. Setting $\xi = 0.50$ (beam mid-span), amplitudes can be calculated for different values of the non-dimensional frequency b.

The frequency response function, spanning the first two natural frequencies, for the mid-point of the beam is shown in Fig. 2.2. (The following parameters apply: $f_1 = 2.9577, f_2 = 1.0000, f_3 = 1.1439, f_4 = 1.0000, f_5 = 3.3368$, $C_1 = 10.0000$, and $C_2 = 10.0000$.)

A comparison between this damped and an undamped version of the same beam is given in Fig. 2.3. Note the shift on the frequencies and changes of amplitude.

For the continuous variation model and using the numerical values given above, the continuously varying functions are shown in Fig. 2.4 (note: $K = 500$).

Assuming a value of 1 for the external forcing $q_1(\xi)$ and using the forced-motion approach [18], the resultant deflections are plotted bellow for two distinct values of the frequency b.

The resonance frequency is taken to occur at $b = 1.55$, as seen in Fig. 2.5.

Amplitudes for the response at the center of the beam can be monitored from Eq. (2.5). The approach leads to the numerical FRF shown in Fig. 2.6. The figure shows the results from the numerical simulation and an overlap of those with the analytical results. Excellent agreement is seen; the first two resonances and amplitude values correspond very well.

From the numerical FRF, the damping ratio of the system, corresponding to the assumed non-dimensional values of damping ($C_1 = 10.0000$, $C_2 = 10.0000$), can be estimated. The method used here is the half-power bandwidth [20], applied to the first mode, which, although only applicable to lightly damped single degree of freedom systems, is frequently applied to well-separated modes of multi-degree of freedom systems. It leads to a ratio of approximately 2%.

[2] www.efunda.com/math/areas/RolledSteelBeamsS.cfm

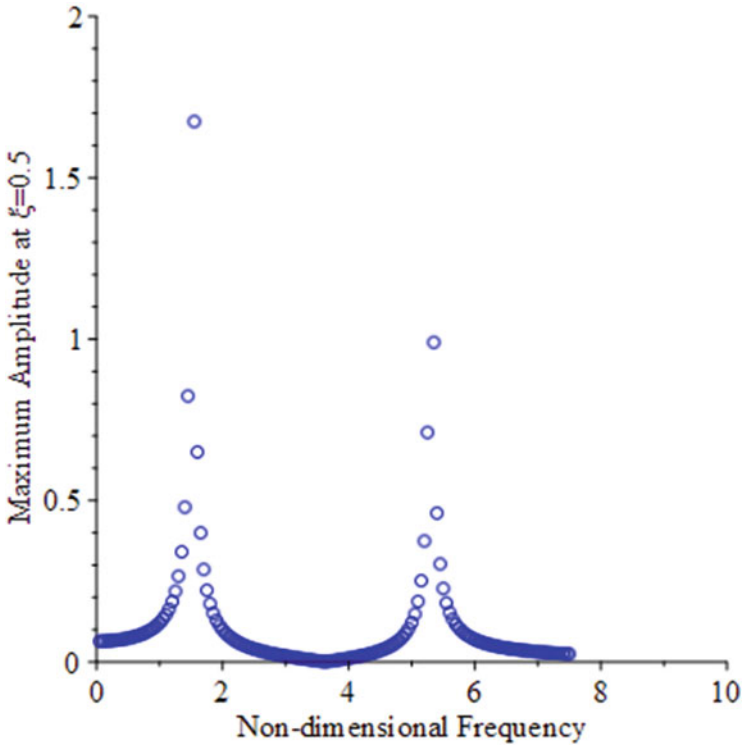

Fig. 2.2 FRF for non-homogeneous Timoshenko beam at mid-point: free/fixed

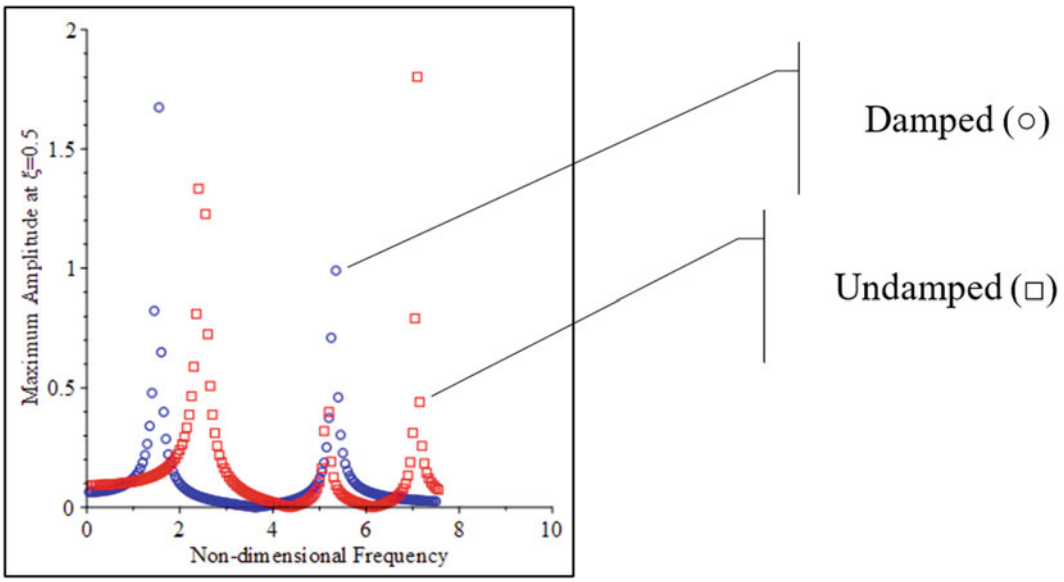

Fig. 2.3 FRFs for damped and undamped non-homogeneous Timoshenko beam: free/fixed

2.4.2 Fixed/Fixed Boundary Conditions

For fixed/fixed conditions, the left-side ($\xi = 0$) constraints change to $Z_1(\xi) = 0$ and $\phi_1(\xi) = 0$, whereas all the other remain the same. The FRF for this case is shown in Fig. 2.7.

A comparison between the damped and undamped results for this beam is given in Fig. 2.8. Note the shift on the frequencies and changes of amplitude.

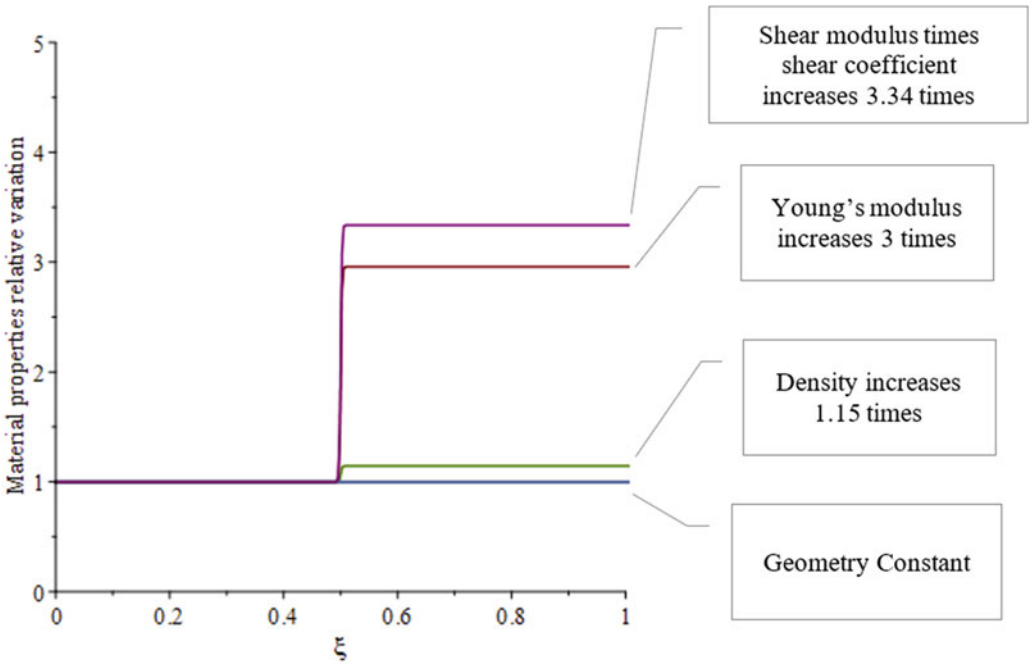

Fig. 2.4 Relative property variation for two-cell Timoshenko beam

Assuming the same external forcing $q_1(\xi)$ as above and using the forced-motion approach, the resultant deflections are shown in Fig. 2.9, for two distinct values of the frequency b.

The resonance frequency is taken to occur at $b = 1.55$.

Monitoring amplitudes at the center of the beam leads to the numerical FRF shown in Fig. 2.10. Results show the numerical simulation and an overlap of these with the analytical results. As in the previous case, excellent agreement is observed.

Consider next a case in which the spatial force is non-constant. For example, a variable force given by the exponential function: $G(\xi) = e^{-\xi^2}$ is assumed. The results can be found using the continuous variation model. The FRFs for this case are seen in Fig. 2.11.

2.5 Assumed Modes Method

In this section, an approach similar to the one described in Ref. [2] is pursued. The solution to Eq. (2.1) is assumed to have the form of a Rayleigh-Ritz expansion:

$$w(x,t) = \sum_{i=1}^{n} \hat{U}_i(t)\eta_i(x), \quad \theta(x,t) = \sum_{i=1}^{n} \hat{V}_i(t)\lambda_i(x) \tag{2.9}$$

where the generalized coordinates $\hat{U}_i$ and $\hat{V}_i$, in the linear combination of shape functions η_i and λ_i, are functions of time.

The shape functions must form a linearly independent set, possessing derivatives up to the order appearing in the strain energy expression for the problem. They also must satisfy the prescribed boundary conditions.

For the undamped case, one can use the expressions for the kinetic energy, strain energy, and the external work done by the transverse loads, for each segment [2], in Lagrange's equations. This leads to a set of n differential equations for the generalized coordinates [21, 22].

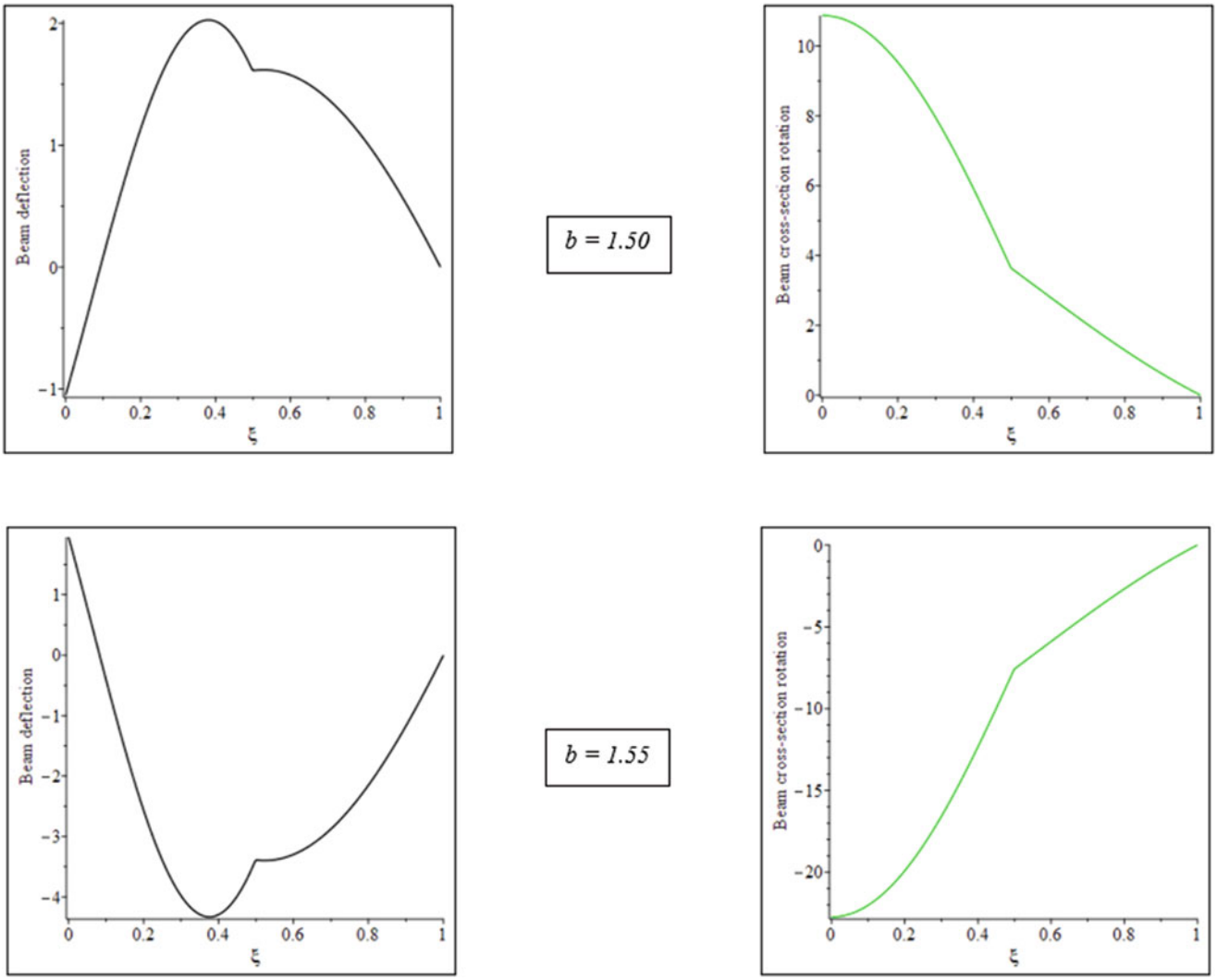

Fig. 2.5 Beam deflections for distinct values of b: free/fixed – first resonance

Then the discrete non-dimensional mass and stiffness matrices [23] can be obtained from:

$$
\begin{aligned}
&M^{\mathrm{I}}{}_{i,j} = \int_0^{\frac{1}{2}} \eta_i \eta_j \, dx + A_r \rho_r \int_{\frac{1}{2}}^{1} \eta_i \eta_j \, dx, \quad M^{\mathrm{II}}{}_{i,j} = \int_0^{\frac{1}{2}} \lambda_i \lambda_j \, dx + I_r \rho_r \int_{\frac{1}{2}}^{1} \lambda_i \lambda_j \, dx, \\
&K^{\mathrm{I}}{}_{i,j} = \int_0^{\frac{1}{2}} \eta_i' \eta_j' \, dx + k_r G_r A_r \int_{\frac{1}{2}}^{1} \eta_i' \eta_j' \, dx, \quad K^{\mathrm{II}}{}_{i,j} = -\int_0^{\frac{1}{2}} \eta_i' \lambda_j \, dx - k_r G_r A_r \int_{\frac{1}{2}}^{1} \eta_i' \lambda_j \, dx, \\
&K^{\mathrm{III}}{}_{i,j} = \int_0^{\frac{1}{2}} \lambda_i' \lambda_j' \, dx + E_r I_r \int_{\frac{1}{2}}^{1} \lambda_i' \lambda_j' \, dx + \int_0^{\frac{1}{2}} \lambda_i \lambda_j \, dx + k_r G_r A_r \int_{\frac{1}{2}}^{1} \lambda_i \lambda_j \, dx, \quad K^{\mathrm{IV}}{}_{i,j} = -\int_0^{\frac{1}{2}} \eta_j' \lambda_i \, dx - k_r G_r A_r \int_{\frac{1}{2}}^{1} \eta_j' \lambda_i \, dx
\end{aligned}
\tag{2.10}
$$

Taking the external transverse loads to be sinusoidal with frequency ν, the generalized external forces can be calculated from:

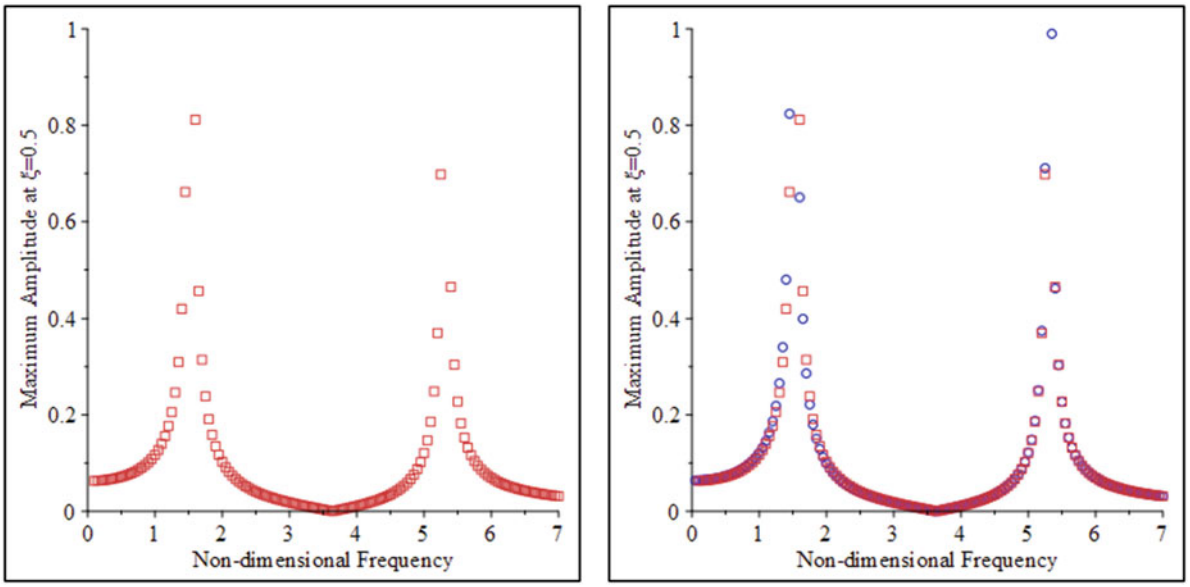

Fig. 2.6 Results comparison: numerical and analytical approaches – free/fixed

$$P_i^{\mathrm{I}} = \left[\int_0^{\frac{1}{2}} p_1 \eta_i dx + \int_{\frac{1}{2}}^{1} p_2 \eta_i \, dx \right] \sin(\nu\tau) \, , \; P_i^{\mathrm{II}} = \left[\int_0^{\frac{1}{2}} p_1 \lambda_i dx + \int_{\frac{1}{2}}^{1} p_2 \lambda_i \, dx \right] \sin(\nu\tau) \tag{2.11}$$

where p_i is the amplitude of the force acting on the i-segment.

Damping is introduced by assuming proportional damping:

$$\begin{bmatrix} [D^{\mathrm{I}}] & [D^{\mathrm{II}}] \\ [D^{\mathrm{IV}}] & [D^{\mathrm{III}}] \end{bmatrix} = \alpha \begin{bmatrix} [M^{\mathrm{I}}] & [0] \\ [0] & [M^{\mathrm{II}}] \end{bmatrix} + \beta \begin{bmatrix} [K^{\mathrm{I}}] & [K^{\mathrm{II}}] \\ [K^{\mathrm{IV}}] & [K^{\mathrm{III}}] \end{bmatrix} \tag{2.12}$$

where α and β are constants of mass and stiffness proportionality, respectively.

The resulting system of equations can be written as:

$$\begin{bmatrix} [M^{\mathrm{I}}] & [0] \\ [0] & [M^{\mathrm{II}}] \end{bmatrix} \begin{Bmatrix} \{\ddot{U}_i\} \\ \{\ddot{V}_i\} \end{Bmatrix} + \begin{bmatrix} [D^{\mathrm{I}}] & [D^{\mathrm{II}}] \\ [D^{\mathrm{IV}}] & [D^{\mathrm{III}}] \end{bmatrix} \begin{Bmatrix} \{\dot{U}_i\} \\ \{\dot{V}_i\} \end{Bmatrix} + \begin{bmatrix} [K^{\mathrm{I}}] & [K^{\mathrm{II}}] \\ [K^{\mathrm{IV}}] & [K^{\mathrm{III}}] \end{bmatrix} \begin{Bmatrix} \{U_i\} \\ \{V_i\} \end{Bmatrix} = \begin{Bmatrix} \{P^{\mathrm{I}}{}_i\} \\ \{P^{\mathrm{II}}{}_i\} \end{Bmatrix} \tag{2.13}$$

The undamped natural frequencies can be evaluated via an eigenvalue problem for the undamped case. The overall system response to external forcing can be estimated through modal analysis.

In order to generate the damping matrix, the constants of mass and stiffness proportionality must be determined. If the modal damping ratios are known, then the constants can be evaluated from:

$$\zeta_i = \frac{\alpha m_{ii} + \beta k_{ii}}{2\sqrt{k_{ii} m_{ii}}} \tag{2.14}$$

where m_{ii} and k_{ii} are coefficients from the modal mass and stiffness matrices, respectively. (See also the approach described in reference [24] for the same purpose, which, for the example considered here, led to similar numerical values.)

Here the modal ratios are not known, but they can be estimated from the previous analytical results. Two modes are needed to calculate α and β. For the free/fixed case, shown in Fig. 2.2, two modes are well defined; then the ratios can be evaluated. The approach used is the half-power bandwidth. For the fixed/fixed case, Fig. 2.7, parameters for the second mode are difficult to evaluate, so, for the numerical example, only the former will be considered.

The procedure requires a choice of shape functions, which are taken to be beam characteristic orthogonal polynomials. They are generated by the Gram-Schmidt process [25] as demonstrated by Bhat [26].

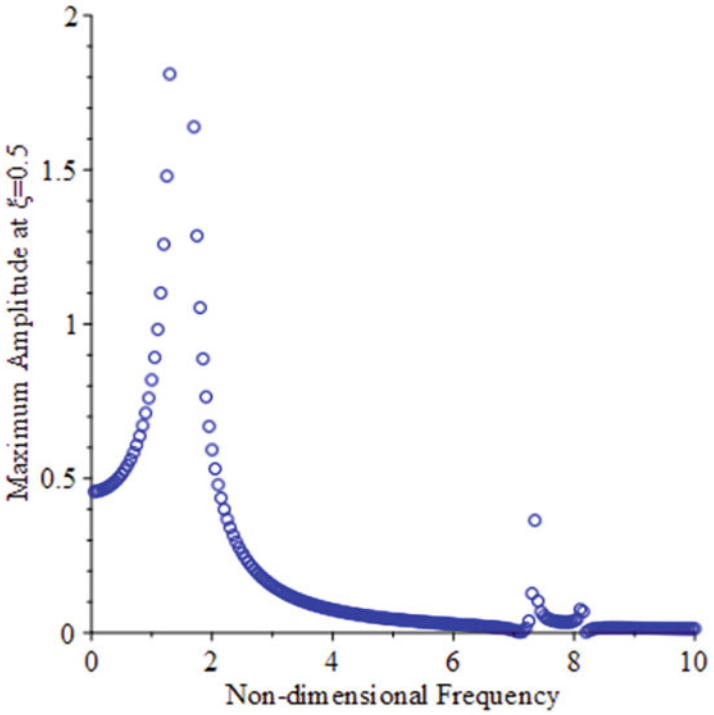

Fig. 2.7 FRF for non-homogeneous Timoshenko beam at mid-point: fixed/fixed

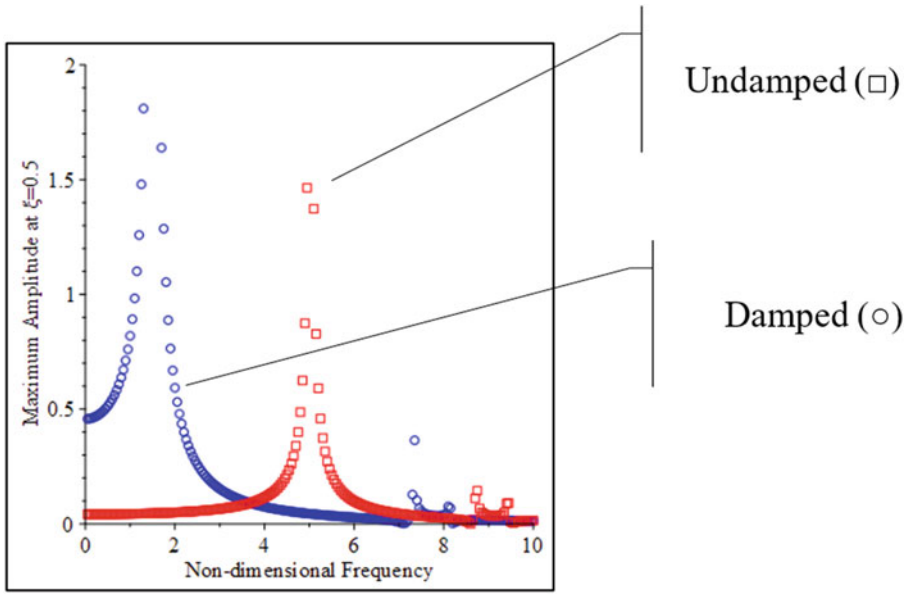

Fig. 2.8 FRFs for damped and undamped non-homogeneous Timoshenko beam: fixed/fixed

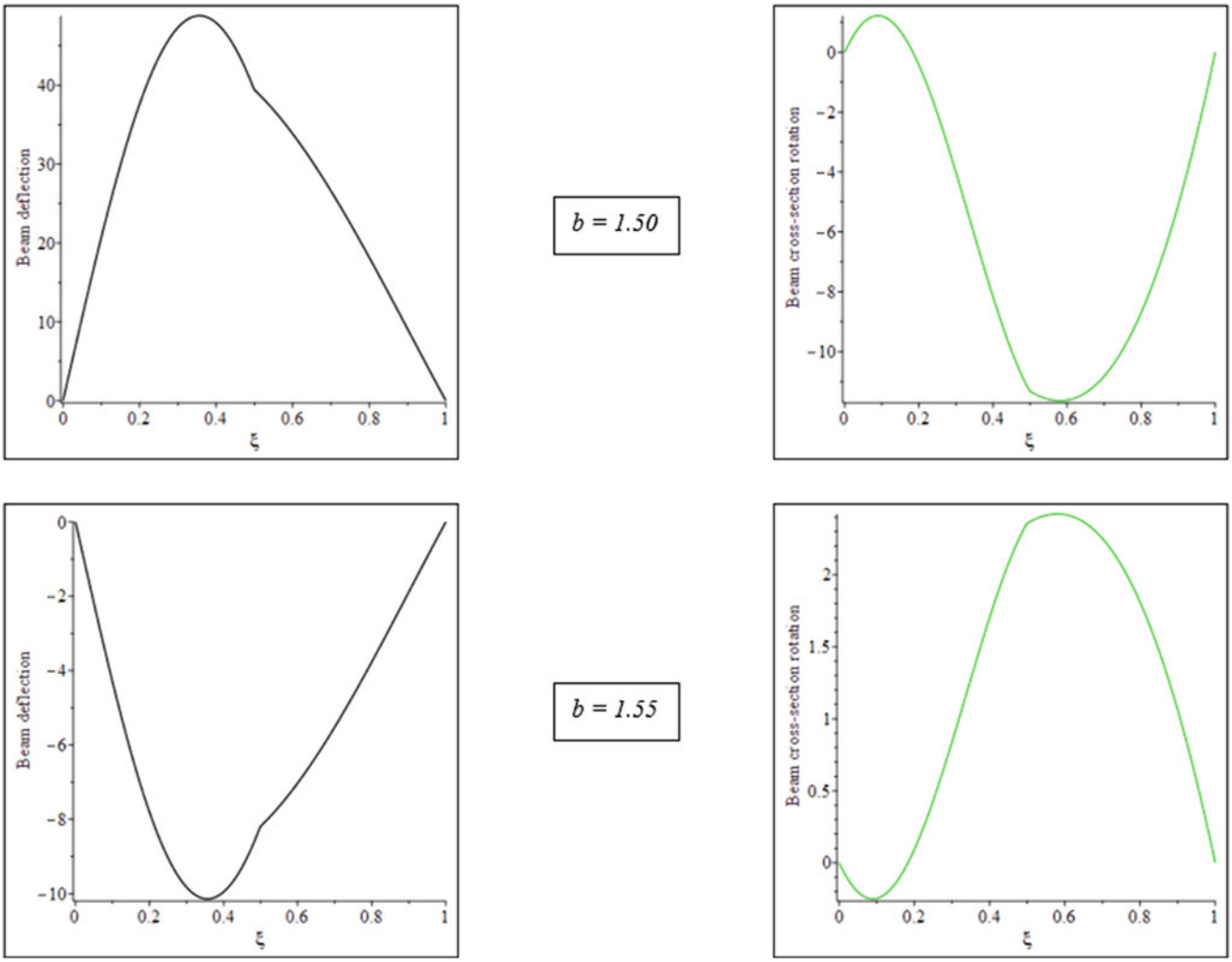

Fig. 2.9 Beam deflections for distinct values of b: fixed/fixed – first resonance

For the free/fixed case, the procedure is described in reference [2]. The first polynomial follows the static deflection of a homogeneous beam, under constant distributed load and with these boundary conditions. In non-dimensional form:

$$\eta_1(x) = s_1\left[\frac{qL}{2kGA}\left(1-\xi^2\right)+\frac{qL^3}{6\mathrm{EI}}\left(\frac{1}{4}\xi^4-\xi+\frac{3}{4}\right)\right], \lambda_1(x) = r_1\left[\frac{qL^3}{6\mathrm{EI}}\left(\xi^3-1\right)\right] \tag{2.15}$$

The constants s_1 and r_1 are chosen such that:

$$\int_0^1 (\eta_k)^2 dx = 1, \int_0^1 (\lambda_k)^2 dx = 1 \tag{2.16}$$

The remainder polynomials are generated by the Gram-Schmidt approach. In addition, the set is also normalized. They are divided by normalization parameters that are taken to be the inverse of the magnitude of their maximum values in the interval $\xi = 0...1$.

Assuming non-dimensional values of damping $C_1 = 0.1$ and $C_2 = 0.1$ ($\zeta_1 \approx 0.0153$, $\zeta_2 \approx 0.0122$), the procedure is tackled using MAPLE®. For 18 polynomials and a non-dimensional time $\tau = 100$, monitoring the amplitudes at $\xi = 0.5$ leads to the results shown in Fig. 2.12. The figure shows a comparison (overlap) between the analytical results and the

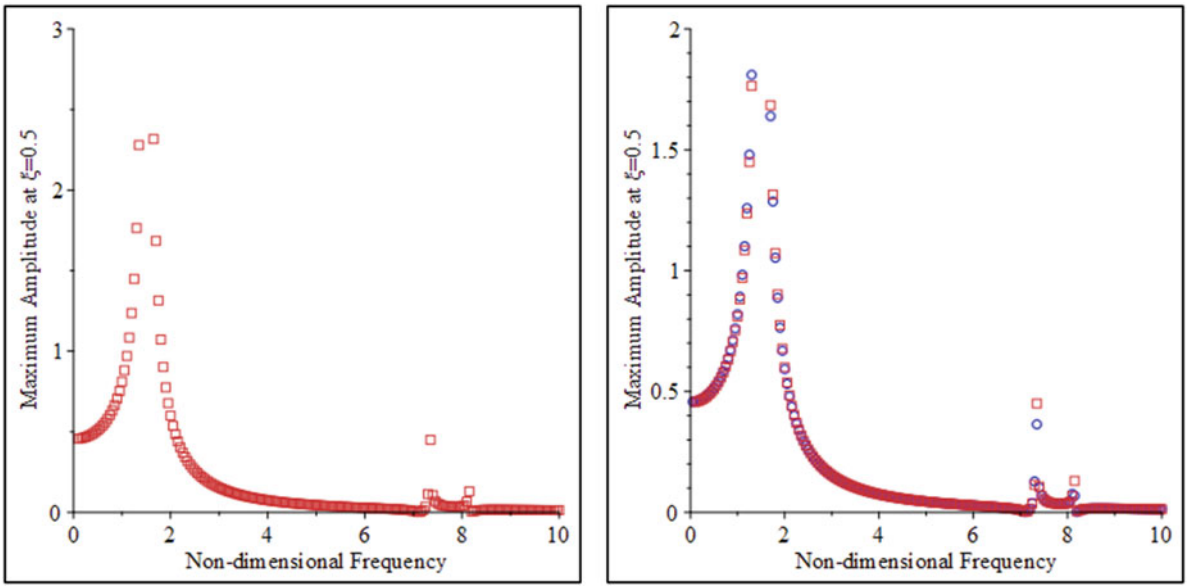

Fig. 2.10 Results comparison: numerical and analytical approaches – fixed/fixed

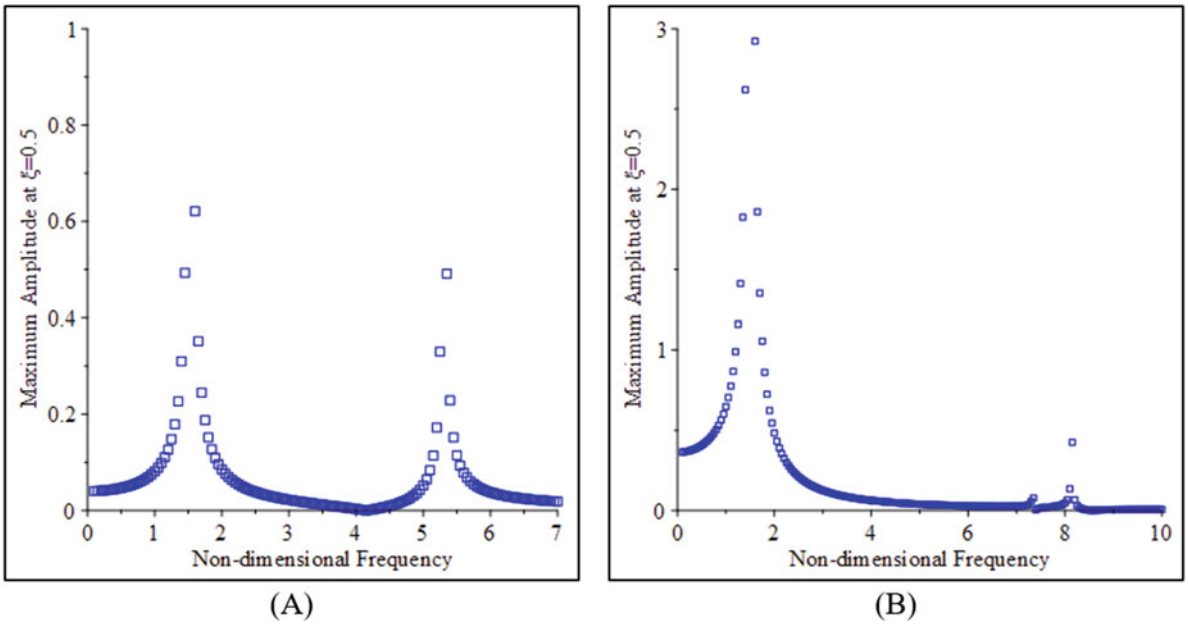

Fig. 2.11 FRFs for exponential force: free/fixed (**a**), fixed/fixed (**b**)

assumed modes approach. The eigensolution gives the following first two frequencies: $\nu_1 = 2.75$ and $\nu_2 = 5.45$, whereas the analytical results are $\nu_1 = 2.50$ and $\nu_2 = 5.20$. The results differ by 10% and 5%, respectively.

2.6 Conclusion

Modeling discrete property variations via continuously varying functions, in conjunction with numerical solutions, has been shown to lead to good results for resonant frequencies and FRFs of viscously damped Timoshenko layered beams subject to harmonic excitation.

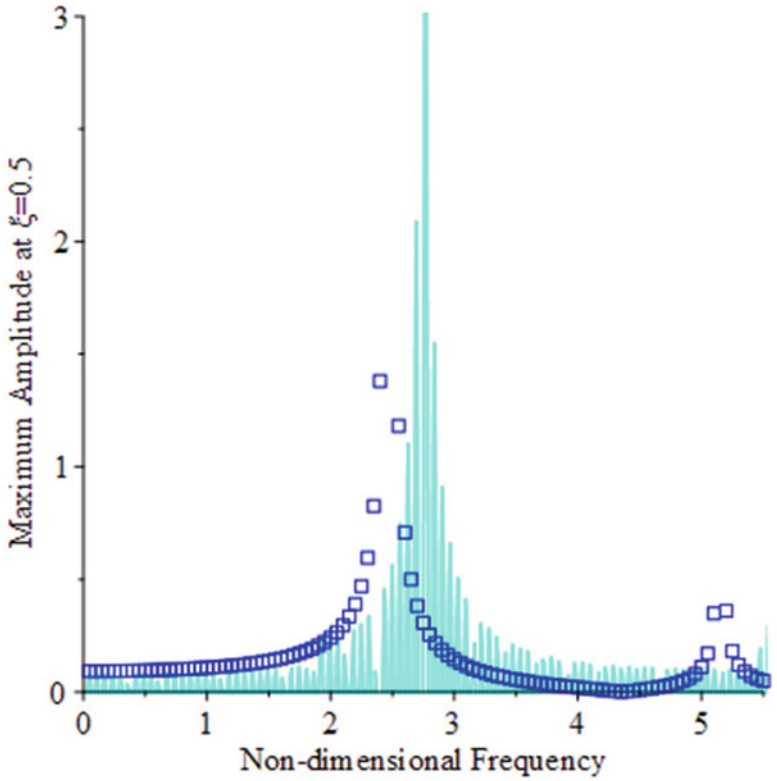

Fig. 2.12 Comparison of FRFs: assumed modes and analytical results – free/fixed

A numerical approach was conducted using MAPLE® software, which shows to lead to accurate solutions based on a comparison to analytical results for specific cases.

Two sets of boundary conditions were studied, namely, free/fixed and fixed/fixed for a uniform two-cell beam made of aluminum and silicon carbide.

Very good agreement was observed for both cases.

The continuous variation approach was used to produce solutions for a case with external spatially varying force, which could be intractable analytically.

Finally, an assumed modes approach was used to estimate the FRF for one of the cases. Good agreement was found with maximum error, when compared to the analytical solution, of 10%.

References

1. Mazzei, A.J., Scott, R.A.: Harmonic forcing of a two-segment Euler-Bernoulli beam. In: Dervilis, N. (ed.) Special Topics in Structural Dynamics, Volume 6: Proceedings of the 35th IMAC, A Conference and Exposition on Structural Dynamics 2017, pp. 1–15. Springer International Publishing, Cham (2017). https://doi.org/10.1007/978-3-319-53841-9_1
2. Mazzei, A.J., Scott, R.A.: Harmonic forcing of a two-segment Timoshenko beam. In: Dervilis, N. (ed.) Special Topics in Structural Dynamics, vol. 5, pp. 1–15. Springer International Publishing (2019). https://doi.org/10.1007/978-3-030-12676-6_3
3. Mazzei, A.J., Scott, R.A.: Harmonic forcing of damped non-homogeneous Euler-Bernoulli beams. In: Epp, D.S. (ed.) Special Topics in Structural Dynamics & Experimental Techniques, vol. 5, pp. 11–23. Springer International Publishing, Cham (2021). https://doi.org/10.1007/978-3-030-47709-7_2
4. Lee, E.H., Yang, W.H.: On waves in composite materials with periodic structure. SIAM J. Appl. Math. **25**, 492–499 (1973). https://doi.org/10.1137/0125049
5. Hussein, M.I., Hulbert, G.M., Scott, R.A.: Dispersive elastodynamics of 1D banded materials and structures: analysis. J. Sound Vib. **289**, 779–806 (2006). https://doi.org/10.1016/j.jsv.2005.02.030
6. Hussein, M.I., Hulbert, G.M., Scott, R.A.: Dispersive elastodynamics of 1D banded materials and structures: design. J. Sound Vib. **307**, 865–893 (2007). https://doi.org/10.1016/j.jsv.2007.07.021

7. Vasseur, J.O., Deymier, P., Sukhovich, A., Merheb, B., Hladky-Hennion, A.C., Hussein, M.I.: Phononic band structures and transmission coefficients: methods and approaches. In: Deymier, P.A. (ed.) Acoustic Metamaterials and Phononic Crystals, pp. 329–372. Springer, Berlin Heidelberg (2013). https://doi.org/10.1007/978-3-642-31232-8_10
8. Hussein, M.I., Leamy, M.J., Ruzzene, M.: Dynamics of phononic materials and structures: historical origins, recent progress, and future outlook. Appl. Mech. Rev. **66**, 040802-040802–38 (2014). https://doi.org/10.1115/1.4026911
9. Capsoni, A., Maria Viganò, G., Bani-Hani, K.: On damping effects in Timoshenko beams. Int. J. Mech. Sci. **73**, 27–39 (2013). https://doi.org/10.1016/j.ijmecsci.2013.04.001
10. Samuels, J.C., Eringen, A.C.: Response of a Simply Supported Timoshenko Beam to a Purely Random Gaussian Process. Purdue Univ Lafayette in Div of Engineering Sciences (1957). https://apps.dtic.mil/dtic/tr/fulltext/u2/134729.pdf
11. Bishop, R.E.D., Price, W.G.: The vibration characteristics of a beam with an axial force. J. Sound Vib. **59**, 237–244 (1978)
12. Kobayashi, K., Yoshida, N.: Unboundedness of Solutions of Timoshenko Beam Equations with Damping and Forcing Terms. https://doi.org/10.1155/2013/435456
13. Lei, Y., Adhikari, S., Friswell, M.I.: Vibration of nonlocal Kelvin–Voigt viscoelastic damped Timoshenko beams. Int. J. Eng. Sci. **66–67**, 1–13 (2013). https://doi.org/10.1016/j.ijengsci.2013.02.004
14. Bozyigit, B., Yesilce, Y., Catal, H.H.: Free flexural vibrations of axially loaded Timoshenko beams with internal viscous damping using dynamic stiffness formulation and differential transformation. In: Kasimzade, A.A., Şafak, E., Ventura, C.E., Naeim, F., Mukai, Y. (eds.) Seismic Isolation, Structural Health Monitoring, and Performance Based Seismic Design in Earthquake Engineering: Recent Developments, pp. 307–328. Springer International Publishing, Cham (2019). https://doi.org/10.1007/978-3-319-93157-9_15
15. Chen, W.-R.: Parametric studies on bending vibration of axially-loaded twisted Timoshenko beams with locally distributed Kelvin–Voigt damping. Int. J. Mech. Sci. **88**, 61–70 (2014). https://doi.org/10.1016/j.ijmecsci.2014.07.006
16. Esmailzadeh, E., Ohadi, A.R.: Vibration and stability analysis of non-uniform Timoshenko beams under axial and distributed tangential loads. J. Sound Vib. **236**, 443–456 (2000). https://doi.org/10.1006/jsvi.2000.2999
17. Cowper, G.R.: The shear coefficient in Timoshenko's beam theory. J. Appl. Mech. **33**, 335–340 (1966)
18. Mazzei, A.J., Scott, R.A.: On the effects of non-homogeneous materials on the vibrations and static stability of tapered shafts. J. Vib. Control. **19**, 771–786 (2013). https://doi.org/10.1177/1077546312438429
19. Chiu, T.C., Erdogan, F.: One-dimensional wave propagation in a functionally graded elastic medium. J. Sound Vib. **222**, 453–487 (1999). https://doi.org/10.1006/jsvi.1998.2065
20. Chopra, A.K.: Dynamics of Structures: Theory and Applications to Earthquake Engineering. Pearson, Hoboken (2017)
21. Craig, R.R., Kurdila, A., Craig, R.R.: Fundamentals of Structural Dynamics. John Wiley, Hoboken (2006)
22. Kelly, S.G.: Advanced Vibration Analysis. CRC/Taylor & Francis, Boca Raton (2007)
23. Eslami, M.R.: Finite Elements Methods in Mechanics. Springer, Cham (2014)
24. Schwarz, B., Richardson, M.: Proportional damping from experimental data. In: Allemang, R., De Clerck, J., Niezrecki, C., Wicks, A. (eds.) Topics in Modal Analysis, vol. 7, pp. 179–186. Springer New York, New York (2014)
25. Chihara, T.S.: Introduction to Orthogonal Polynomials. Gordon and Breach, London (1978). https://doi.org/10.1007/978-1-4614-6585-0_17
26. Bhat, R.B.: Transverse vibrations of a rotating uniform cantilever beam with tip mass as predicted by using beam characteristic orthogonal polynomials in the Rayleigh-Ritz method. J. Sound Vib. **105**, 199–210 (1986). https://doi.org/10.1016/0022-460X(86)90149-5